Ab initio electronic structure calculations for metallic intermediate band formation in photovoltaic materials

P. Wahnón[1,2] and C. Tablero[1]
[1]*Instituto de Energía Solar, ETSI Telecomunicación, Universidad Politécnica de Madrid, 28040 Madrid, Spain*
[2]*Departamento de Tecnologia Especiales Aplicadas a la Telecomunicación, ETSI Telecomunicación, Universidad Politécnica de Madrid, 28040 Madrid, Spain*
(Received 27 April 2001; revised manuscript received 10 July 2001; published 10 April 2002)

A metallic isolated band in the middle of the band gap of several III-V semiconductors has been predicted as photovoltaic materials with the possibility of providing substantially enhanced efficiencies. We have investigated the electronic band structures and lattice constants of Ga_nAs_mM and Ga_nP_mM with M=Sc, Ti, V, and Cr, to identify whether this isolated band is likely to exist by means of accurate calculations. For this task, we use the SIESTA program, an *ab initio* periodic density-functional method, fully self consistent in the local-density approximation. Norm-conserving, nonlocal pseudopotentials and confined linear combination of atomic orbitals have been used. We have carried out a case study of Ga_nAs_mTi and Ga_nP_mTi energy-band structure including analyses of the effect of the basis set, fine *k*-point mesh to ensure numerical convergence, structural parameters, and generalized gradient approximation for exchange and correlation corrections. We find the isolated intermediate band when one Ti atom replaces the position of one As (or P) atom in the crystal structure. For this kind of compound we show that the intermediate band relative position inside the band gap and width are sensitive to the dynamic relaxation of the crystal and the size of the basis set.

DOI: 10.1103/PhysRevB.65.165115 PACS number(s): 71.20.Nr, 71.28.+d, 71.55.−i, 81.05.−t

I. INTRODUCTION

The application of *ab initio* electronic structure calculations for designing materials with improved optoelectronic properties for microelectronic devices is currently a very useful emerging tool. The aim of this paper is to investigate theoretically, with a first-principles technique, a material able to produce a photovoltaic device with a significant enhancement of the theoretical limiting efficiency of conventional Si solar cells.

Recently, Luque and Martí[1] have proposed the feasibility of a *third generation* photovoltaic solar cell concept with efficiencies exceeding considerably the thermodynamic limits set by Shockley and Queisser[2] in 1961. For this, just as plants break the water molecule in the chlorophyll function, two photons are used to produce an electron-hole pair of high free energy using intermediate bands (IB) situated in the semiconductor band gap, as an intermediate step in this operation. Lower-energy photons may pump electrons to the IB from the valence bands (VB), and from the IB to the conduction bands (CB). In order to facilitate photon absorption to and from this IB, they must contain filled and empty states.[3]

It is important to state that the IB must be isolated from the ordinary VB and CB. For this, zero density of states, gaps must be formed so that no band in the IB can interfere with either the CB or the VB in any of the reciprocal lattice directions. Otherwise a fast deexcitation would occur as a result of interaction with phonons.[4]

Our purpose is to find, by means of first-principles calculations, intermediate metallic band formation isolated in the band gap of III-V semiconductor compounds such as GaAs and GaP by adding different substitute elements in order to form a ternary alloy. Because their band-gap properties are extensively studied and the technologies are well tested, we choose these host semiconductors to design the suitable alloys. Moreover, looking at the theoretical limits of the efficiencies, GaP seems to be preferred with a gap close to the gap values corresponding to the maximum of the efficiency curve.[1] Regarding the third element, a large number of test calculations on different possible substitutes has been made. Even though we are looking for an intermediate isolated band, not a level, preliminary band diagram calculations have been made taking into account the relative position of the measured ionization energies of different impurities in the host semiconductors. Further analysis of detailed *ab initio* quantum-mechanic calculations made for semiconductor alloy compounds with several transition element substitutes such as Sc, Ti, V, Cr, . . . , shows a similar band diagram picture with semiconductor characteristics. This behavior highlights the possibility of covalent hybridized bonding between some valence electrons of the transition metal and the host semiconductor nearest atoms, due to the relative localized character of the $3d$ valence electrons. Comparison of the results of all the different transition-metal alloys used, shows that both Ti and Sc present an isolated half metallic intermediate band for the two host semiconductors PGa and AsGa. Because Ti is more well known in technological device circles, we choose it as a good candidate for detailed study. When Ti atoms with four valence electrons substitute a given position in the crystalline structure of one III-V semiconductor, one additional electron or a hole is produced leading to a band with metallic characteristics. Therefore, Fermi energy will be located in this case inside the IB.

To achieve this objective, a very accurate and detailed calculation needs to be made for the band diagram and material parameter.[5] As said before, first-principles methods have become a widespread tool for studying the microscopic aspect of condensed systems. In these methods the electronic

ground state is evaluated without requiring empirical modeling of the interatomic interactions. However, the use of *ab initio* methods for band-structure calculations requires massive computing resources. For systems of such complexity the adoption of efficient methods is necessary. In the last few decades, the density-functional theory (DFT) has made a great impact on the computational electronic structure of molecules and solids,[6,7] mainly because of its ability to include part of the effect of electron exchange and correlation without significantly increasing the computational cost.

In this paper we report the detailed calculations of the microscopic properties of Ga_4TiAs_3 and Ga_4TiP_3 compounds in bulk conditions through the use of an efficient *ab initio* computed code, known as SIESTA.[8] This code is based on the density-functional theory combining the use of a localized linear combination of atomic-orbitals basis set for the description of valence electrons and norm-conserving nonlocal pseudopotentials for the atomic core. The self-consistent Kohn-Sham equations are solved in this code within the local density and in the generalized gradient correction approximations of DFT.

Because, so far, these alloys have not been studied,[9] our results on the electronic structure of the half filled intermediate band formation in the band gap of the semiconductor are in the nature of a prediction. We focus our attention mainly on this fact, because our work was motivated by the search for photovoltaic materials with the relevant technological characteristics already described. For this, an extended behavior comparison of other alloy semiconductor systems, made with different transition elements of the same series as Ti is also shown. Then we analyze for the two systems, Ga_4TiAs_3 and Ga_4TiP_3, the sensitivity of intermediate band stability according to basis set convergence. We present our detailed results in terms of massive band structure, bonding properties, lattice parameter, density of states (DOS), Mulliken population analysis, and charge density.

This paper is organized as follows: in Sec. II, we give a brief description of the method and computational details, in Sec. III, we present results and the discussion of the electronic properties and Sec. IV contains the conclusions.

II. METHOD AND COMPUTATIONAL DETAILS

Kohn-Sham density-functional theory,[10] is a very popular tool for electronic structure calculations of ground-state properties in bulk materials, surfaces, and nanostructures. In particular, the approximation based on the local density for the exchange-correlation potential[11] has generally been accurate enough to give properties obtained from total-energy calculations.

In our paper, we use for the exchange-correlation potential both the local-density approximation (LDA) in the Ceperley-Alder form[12] with the parametrization fitting given by Perdew and Zunger,[13] as well as the generalized gradient approximation (GGA) corrections[14–17] in the form of Perdew, Burke, and Ernzerhof (PBE).[18] The latter approximation is constructed in a simpler functional form than the traditional Burke, Perdew, and Wang[19] functional, which has been applied to a variety of problems in solids and surfaces.

The calculations of the self-consistent nonpolarized Schroedinger equation for the one particle problem have been carried out in this paper with the direct diagonalization method of the SIESTA code program.[8] This code makes all the calculations projecting electron wave functions and density onto a real space grid.

In order to get smooth valence wave functions a nonlocal and norm-conserving pseudopotential is used to replace the core electrons. Pseudopotentials are constructed using the Trouiller and Martins scheme[20] to described the valence electron interactions with the atomic core and the nonlocal components of the pseudopotential are expressed in the fully separable form of Kleinman and Bylander.[21,22]

In this paper, the core electrons were taken to be the $3p$ electrons and below for Sc, Ti, V, and Cr, $2p$ and below for P, and $3d$ and below for Ga and As. Pseudopotentials were generated from the neutral atoms and optimization of all orbitals was carried out. Nonlinear partial core corrections were also included in the test calculations.

Regarding the basis set for the description of valence electrons, the code program uses a localized linear combination of finite-range numerical pseudoatomic wave functions of the Sankey and Niklewski type.[23] The local basis set is used to improve the computational efficiency of the electronic structure calculations,[24] although the convergence of the localized basis set is more difficult than with plane waves because of the number of parameters to be checked. Specifically, this type of short-range basis vanishes beyond a certain confinement radius defined by an orbital energy shift parameter.[25] In our calculations, the shift-energy parameter for the finite range of the pseudoatomic orbitals ΔE_{PAO} was tested for these systems to ensure the energy convergence. ΔE_{PAO} were all chosen to be less than 0.05 eV for both the exchange-correlation potential LDA and GGA used. The values obtained for the orbital-dependent cutoff radius of all PAO are summarized in Table I.

In this paper, several sets of atomic orbital bases of different size and qualities were used in the detailed calculations for all the atoms.[26,27] Calculations with single ζ (SZ: one *s* and three *p* orbitals for Ga, As, and P and one *s* and five *d* orbitals for Ti), and double ζ (DZ: the valence orbitals are split into two components), have been used. Convergence tests with polarization functions for the DZ basis set (DZP: adding five *d* for Ga, As, and P and three *p* orbitals for Ti) were also done in order to obtain the required accuracy.

Our calculations were carried out specifically for two systems, Ga_nAs_mTi and Ga_nP_mTi, with an eight-atom simple cubic unit cell, where a Ti atom replaces one atom of As or P, respectively. Due to the relative localized nature of the $3d$ Ti electrons we could expect the formation of some covalent bonding between the Ti and the others atoms, and do not expect much distortion in the crystal structure. The character of the bonding will be further analyzed by plotting the distribution of the charge density. A crystal structure model equivalent to that of the host semiconductors is used in all calculations. This model is illustrated in Fig. 1 and is assumed to have the smallest possible unit cell and the highest symmetry. A very fine *k*-point sampling of the Brillouin zone was tried with an increasing density of points up to 132 to

TABLE I. Orbital dependent cuttoff radius in Bohr units for all pseudo atomic orbitals (PAO) used in the calculations for the GGA and LDA exchange and correlation potential used with an energy shift of 50 meV.

Atom	PAO	$r_c^{(GGA)}$	$r_c^{(LDA)}$
As	4*s*	5.49	5.49
	4*s*'	4.07	4.07
	4*p*	7.23	7.23
	4*p*'	4.84	4.84
Ga	4*s*	6.62	6.46
	4*s*'	4.97	4.97
	4*p*	9.17	9.17
	4*p*'	6.46	6.46
P	3*s*	5.43	5.43
	3*s*'	3.97	3.97
	3*p*	6.97	6.97
	3*p*'	4.56	4.61
Ti	4*s*	8.88	8.66
	4*s*'	7.27	7.18
	3*d*	6.10	6.10
	3*d*'	3.10	3.10

provide a sufficiently accurate description of the electronic ground state. The degree of convergence was checked for all calculations in the eight-atom cell chosen. In our results we obtain convergence of both the total energies and Kohn-Sham eigenvalues better than 0.04 eV.

Relaxation of the ions to mechanical equilibrium, to get the optimization of the geometry, was achieved in all calculations by the conjugate gradient minimization of the total energy with respect to the ionic positions. In the code program, the atomic forces are obtained using a variation of the Hellman-Feynman theorem including Pulay corrections[8] to account for the local character of the basis set. In our case, the residual atomic forces were generally less than 0.04 eV $Å^{-1}$ and the stress tolerance less than 0.1 G Pa.

Our goal in this paper is the prediction of the properties of two compounds: Ga_4TiAs_3 and Ga_4TiP_3, with specific lattice constants obtaining after atomic relaxation, band-gap values,

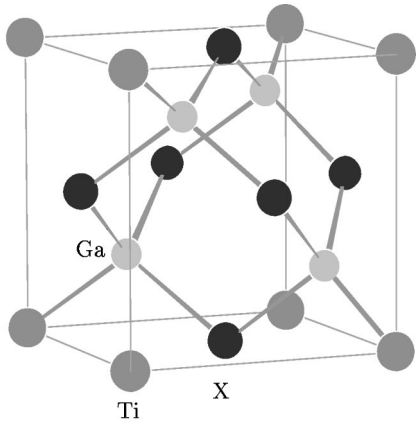

FIG. 1. The cubic crystal structure with $X = As, P$.

and band structures, which have not yet been synthesized. Test calculations were made on AsGa and PGa with the same eight-atom simple cubic unit cell to compare them with experimental values of energies and structure parameters.

III. RESULTS AND DISCUSSION

A. Crystal Structure

The ground-state properties of ternary alloy structures are obtained by the minimization of the total energy with respect to the base atoms and the lattice parameters.

Convergence behavior of ground-state total energies versus increasing size and quality of basis set are displayed for the two alloys Ga_4As_3Ti and Ga_4P_3Ti in Fig. 2. It is shown from the figure, that a basis set of the size of DZ for all atoms ($n=6$ in the figure), is sufficiently converged, especially in the case of the Ga_4P_3Ti compound. The maximum energy differences between the minimal $n=2$ basis set (SZ) and the extended $n=7$ basis set (DZP) amount to 1.46 eV for Ga_4P_3Ti and 1.40 eV. for Ga_4As_3Ti, respectively.

The shift-energy parameter ΔE_{PAO} for the finite range of the pseudoatomic orbitals was also tested for both systems within a range of 0.2–0.01 eV to ensure the energy convergence. We illustrate in Fig. 3 the great stability of the intermediate bandwidth and the two band-gap values in the large range of the ΔE_{PAO} studied.

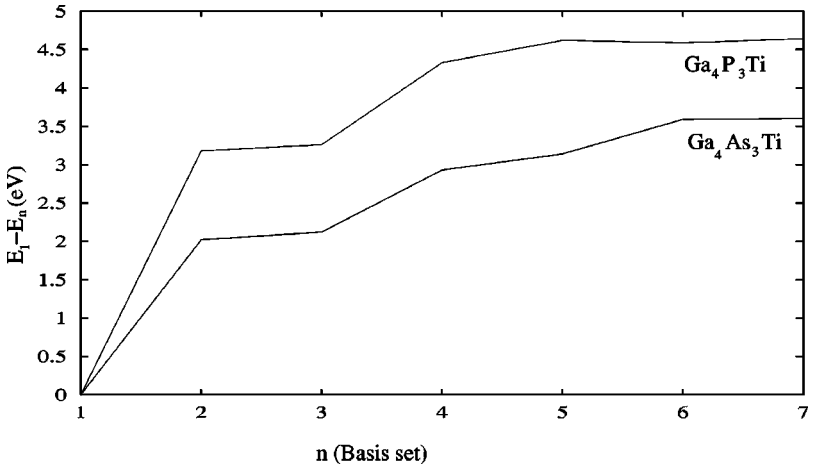

FIG. 2. Energy convergence versus basis set size as defined in Tables IV and V.

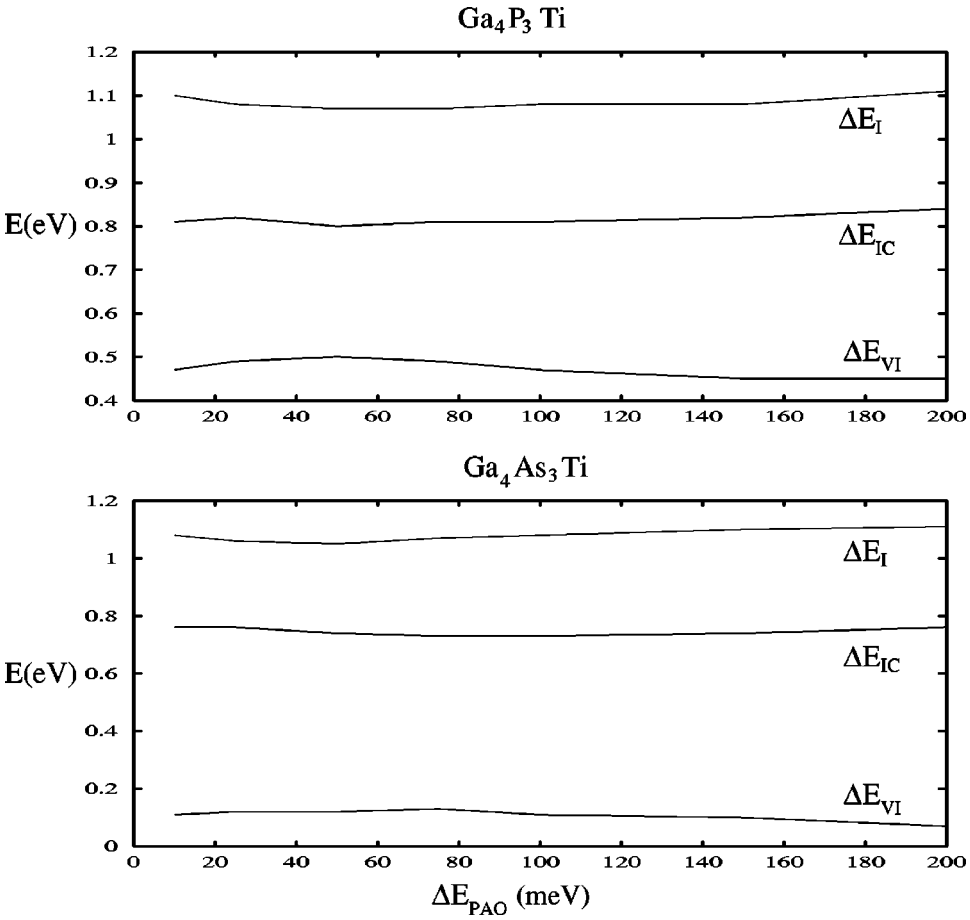

FIG. 3. Convergence of energy properties for Ga_4P_3Ti and Ga_4As_3Ti versus energy shift parameter. ΔE_{VI} is the valence-intermediate band gap, ΔE_{IC} is the intermediate-conduction band gap, and ΔE_I is the intermediate bandwidth.

The cohesive energy of the compounds, as a measure of the strength of the forces which bind atoms together in the solid state,[28] are calculated as the difference between the computed atomic energies of the pure constituents and the total energy of the compound from the relation

$$E_{coh}=(E_{Ti}+3E_X+4E_{Ga})-E_{TiGa4X3}$$

$$\text{with} \quad X=\text{As or P}.$$

The calculated values of the lattice parameters and the cohesive energies of the two compounds obtained after atomic and lattice relaxation using GGA (PBE) are shown for different qualities of basis sets in Tables II and III, and compared one of the basis set with the LDA results. We also show a comparison for one calculation for each system made with fixed lattice constants, corresponding to those of substrate semiconductors, PGa and AsGa, before obtaining the dynamical relaxation of the crystal. We note that results coming from the reduced basis set (SZ-GGA) yield, systematically in both systems, cohesive energies lower than the converged extended basis set (DZ-GGA), suggesting a stronger binding for the latter. This effect of the basis size amounts to 4.6% for Ga_4TiAs_3 and 4.4% for Ga_4TiP_3, improving cohe-

TABLE II. Cohesive properties of cubic $TiGa_4As_3$. We display lattice constants, ground-state total and cohesive energies, and a comparison with experimental results for AsGa. The first column indicates the type of basis set and exchange potential used in the calculations.

	E(eV)	E_{coh}(eV)	a(Å)
SZ-LDA	−851.10	33.33	5.94
SZ-GGA[a]	−837.35	26.93	5.65
SZ-GGA	−839.43	29.01	6.11
DZ-GGA	−840.83	30.41	6.02
Experiment (GaAs)[b]		26.08	5.65

[a]Calculation performed with fixed lattice constant.
[b]Reference 31.

TABLE III. Cohesive properties of cubic $TiGa_4P_3$. We display lattice constants, ground-state total and cohesive energies, and a comparison with experimental results for PGa. The first column indicates the type of basis set and exchange-potential used in the calculations.

	E(eV)	E_{coh}(eV)	a(Å)
SZ-LDA	−873.89	35.32	5.76
SZ-GGA[a]	−860.99	27.31	5.45
SZ-GGA	−864.17	30.49	5.97
DZ-GGA	−865.58	31.90	5.88
Experiment (GaP)[b]		28.48	5.45

[a]Calculation performed with fixed lattice constant.
[b]Reference 32.

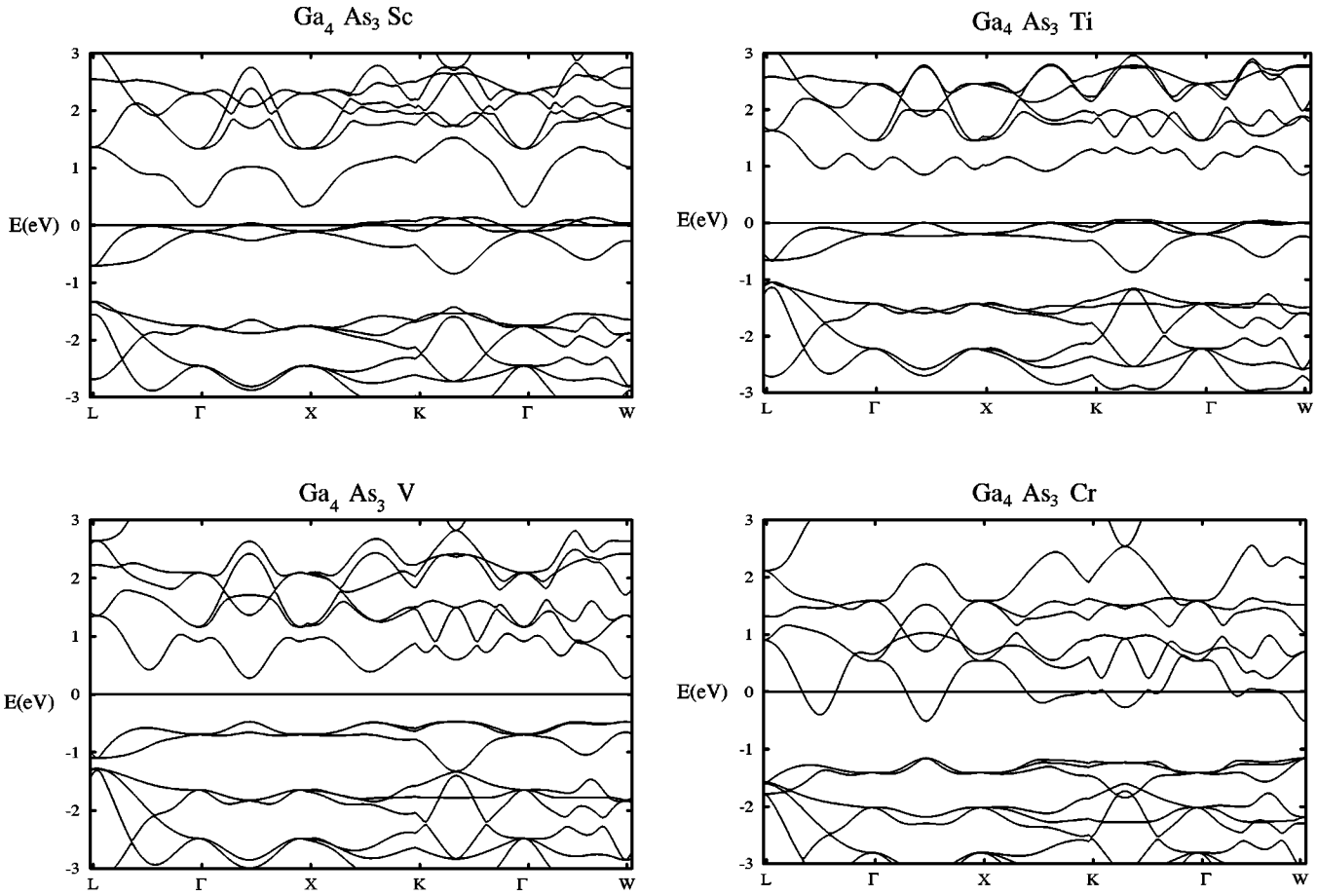

FIG. 4. The bulk electronic band structure for Ga_4As_3M series with $M=$ Sc, Ti, V, and Cr in the DZ-GGA calculations after dynamical relaxation. The Fermi level of the compound has been set at the energy zero. The diagram is displayed in the main directions of the corresponding first Brillouin zone of a fcc structure.

sive energies, and 1.4 and 1.5 %, respectively, for lattice parameters. For this type of study the cohesive energy is more descriptive than the total valence energy because the latter includes a large contribution from electronic states that are not significant for the bonding.

The general feature of bulk semiconductors[29,30] is that the LDA often yields a very accurate lattice constant but the GGA that favors density inhomogeneity, predicts a better binding energy and other energy parameters which, in LDA, are overestimated. In our case, it is evident from Tables II and III, that our best results for the Ga_4TiAs_3 and Ga_4TiP_3 compounds are for the LDA lattice parameter 5.94 and 5.76 Å, and for DZ-GGA cohesive energy 30.41 and 31.90 eV, respectively. These positive values of the cohesive energies are consistently comparable to the experimental values of AsGa and PGa, giving a very reasonable expectation for the stability of the alloys. Furthermore, the values of the DZ-GGA (LDA) lattice parameters for both alloys, 6.02/5.88 Å (5.94/5.76 Å), are not very different 4.96/5.51% (4.9/5.4%), respectively, to those corresponding to the experimental AsGa/PGa[31,32] parent substrates 5.65/5.45 Å. As a reference, the calculated lattice parameters DZP-GGA (LDA) for the parent semiconductors, after atomic and lattice relaxation, are close especially in the case of PGa and give 5.84/5.64 Å (5.68/5.44 Å). Theses values suggest the compatibility of lattice size for the growth of the alloys on the corresponding substrates.

In addition, we also analyze the bond-length distribution within the unit cell used in the calculations after dynamical relaxation. The interatomic distances for the two different calculation models DZ-GGA/LDA, are, respectively, for the Ga_4TiAs_3 system: $r_{Ga\text{-}As}=2{,}75/2{,}59$, $r_{Ti\text{-}Ga}=2{,}82/2{,}63$, and $r_{Ti\text{-}As}=4{,}52/4{,}24$ Å and for the Ga_4TiP_3 system: $r_{Ga\text{-}P}=2{,}61/2{,}52$, $r_{Ti\text{-}Ga}=2{,}72/2{,}62$, and $r_{Ti\text{-}P}=4{,}30/4{,}16$ Å. The distances Ga-As and Ga-P in the alloys are bigger than the corresponding experimental GaAs and GaP host semiconductors: $r_{Ga\text{-}As}=2{,}45$, $r_{Ga\text{-}P}=2{,}36$ Å, in the same way as the related lattice parameters are. This increase could be explained due to the formation of weaker bonds between the Ti atom and the first and second neighboring atoms allowing the formation of the intermediate band.

B. Band Structures and Properties

The *ab initio* energy-band diagrams of semiconductor alloys Ga_4As_3M and Ga_4P_3M with $M=$ Sc, Ti, V, and Cr, for eight-atom cubic supercells calculated under the previously explained conditions for dynamically atomic relaxed DZ-GGA, are shown for the first Brillouin zone in Figs. 4 and 5. The Fermi-level position is also shown in all cases. Close

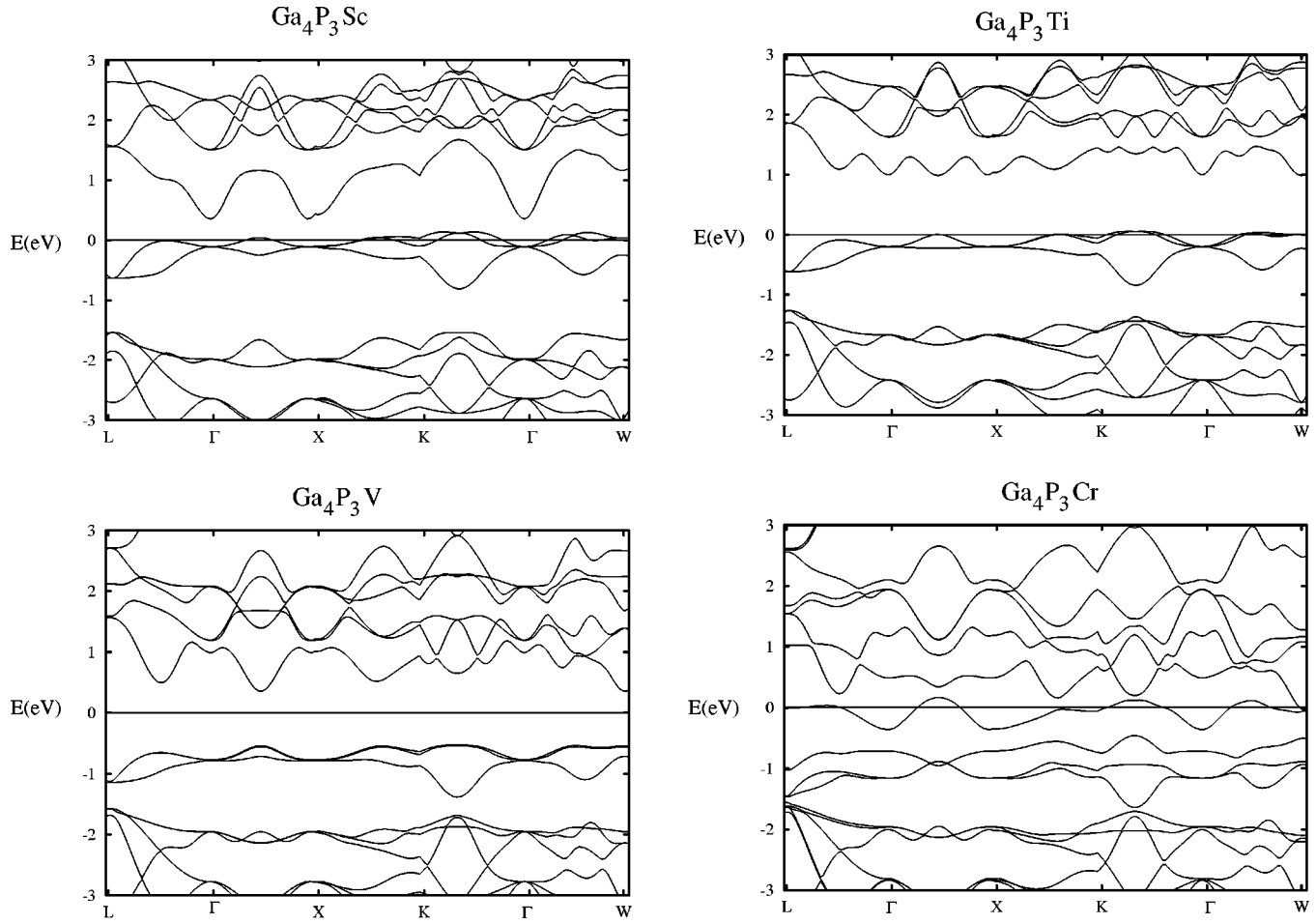

FIG. 5. The bulk electronic band structure for Ga_4P_3M series with $M=$ Sc, Ti, V, and Cr in the DZ-GGA calculations after dynamical relaxation, like in Fig. 4.

inspection of the band diagrams shows that all alloy compounds exhibit semiconductor behaviors with a very similar qualitative structure for band diagrams. However, only four of them, those corresponding to the Sc and Ti substitutes present an isolated, partially filled band within the band gap of the host semiconductors. In the Sc substitution cases two holes are produced leading to the isolated half metallic IB while for Ti cases only one hole is produced in the isolated IB.

As previously stated, we chose the Ti atom as a substitute in both host semiconductors, PGa and AsGa, for detailed studies. In these cases, the states responsible for IB formation are 14, 15, and 16 in the total systems. We obtained the isolated IB with very similar features in the two alloys, Ga_4As_3Ti and Ga_4P_3Ti, for all cases studied with all different basis sets and the two types of exchange correlation potentials.

These narrow IB are fairly separated from a quasidegenerate higher state in the valence band by a direct gap close to the *K* point specified and from the lower state of the conduction band near the *X* point by an indirect gap. We notice that for the indirect transition, several locations compete for the minimum of the conduction band whereas direct transitions are well localized in the reciprocal lattice. In Fig. 6 we show, for atomic relaxed DZ-GGA calculations, the enlarged band structure of (a) Ga_4As_3Ti and (b) Ga_4P_3Ti around the Fermi level and in a smaller part of the Brillouin zone. The states responsible for direct transitions have been labeled 1 and 2, and those of the indirect transitions, 3 and 4. In semiconduc-

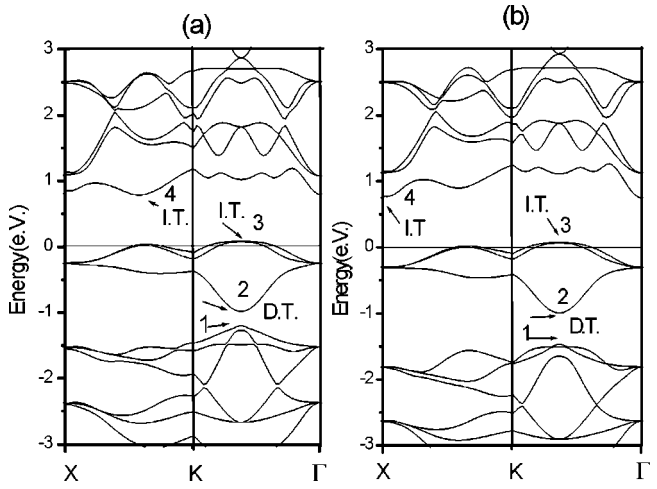

FIG. 6. Band structures around the Fermi level for (a) $TiGa_4As_3$ (b) $TiGa_4P_3$ using DZ-GGA calculations and the same ZB notation as Figs. 4 and 5. The states of interest for transitions are labeled.

TABLE IV. Energy properties for $TiGa_4As_3$ calculated all in eV for a different type of basis set and exchange correlation potential. ΔE_{VI} is the gap valence-intermediate band, ΔE_I is the width of the intermediate band, ΔE_{IC} is the gap intermediate-conduction band, ΔE_{VC} is the gap valence-conduction band, and ΔE_{FV} is the difference between Fermi energy and top valence band energy.

	ΔE_{VI}	ΔE_I	ΔE_{IC}	ΔE_{VC}	ΔE_{FV}
SZ-LDA	0.12	1.05	0.74	1.91	1.11
SZ-GGA[a]	0.44	1.08	0.81	2.33	1.43
SZ-GGA	0.21	0.89	0.72	1.82	1.05

[a]Calculation performed with fixed lattice constant.

tors, density-functional calculations provide a good description of the experimental structure of band diagrams, both for the valence and the conduction band, except for a rigid shift in the energy position of the conduction band. This is the band-gap problem.[33] In our case, this feature means an enhancement of two direct and indirect gaps, leading predictably to keeping the IB more isolated as we look for it.

The values for these two gaps and the width of the IB are summarized for every system studied in Tables IV to VII. To facilitate the comparison of the results, we define ΔE_{VI} as the energy difference between points 1 and 2 labeled in Fig. 6, ΔE_I the energy difference between 2 and 3, and ΔE_{IC} the energy difference between 3 and 4. ΔE_I corresponds to the maximum width value of the intermediate band and ΔE_{VC} is the maximum energy difference between the top valence band and the bottom of the conduction band. In these tables we also define ΔE_{FV} as the difference between the Fermi and the top valence-band energies.

We note that magnitudes of the different gap values do not differ very much in each compound in spite of the various exchange-correlation potential approximations (LDA, GGA) and quality of basis set used, which obviously assess for the stability of the IB formation. In particular, Tables VI and VII show the evolution of the different band-gap parameters with the increasing size of the basis set for GGA calculations. The stability of the energy differences is reached for the quality of basis set close to DZ, especially for Ga_4P_3Ti compound.

We also note that in all cases studied for these two compounds, the corresponding first gap ΔE_{VI} is a direct gap whereas the second gap ΔE_{IC} is an indirect gap. This characteristic makes both compounds Ga_4As_3Ti and Ga_4P_3Ti materials with indirect total band gaps, however the situation for the corresponding parent semiconductors is direct band gap for AsGa and indirect bandgap for PGa.

TABLE V. Energy properties for $TiGa_4P_3$ calculated all in eV for a different type of basis set and exchange correlation potential. Same legend as in Table IV.

	ΔE_{VI}	ΔE_I	ΔE_{IC}	ΔE_{VC}	ΔE_{FV}
SZ-LDA	0.50	1.07	0.80	2.37	1.49
SZ-GGA[a]	0.72	1.13	0.94	2.79	1.75
SZ-GGA	0.47	0.87	0.82	2.16	1.28

[a]Calculation performed with fixed lattice constant.

TABLE VI. Energy properties convergence versus basis set size in GGA calculations for $TiGa_4As_3$. Same legend as in Table IV.

n	Basis set(Ti/Ga/As)[a]	ΔE_{VI}	ΔE_I	ΔE_{IC}	ΔE_{VC}	ΔE_{FV}
1	SZ/SZ/SZ[b]	0.44	1.08	0.81	2.33	1.43
2	SZ/SZ/SZ	0.21	0.89	0.72	1.82	1.05
3	SZP/SZ/SZ	0.23	0.88	0.65	1.76	1.06
4	SZP/SZP/SZP	0.31	0.86	0.46	1.64	1.10
5	DZP/SZP/SZP	0.25	0.91	0.56	1.72	1.10
6	DZ/DZ/DZ	0.11	1.06	0.62	1.79	1.11
7	DZP/DZ/DZ	0.12	1.06	0.59	1.77	1.12

[a]SZ: single ζ; DZ: double ζ; SZP: SZ with polarization; DZP: DZ with polarization.

[b]Calculation performed with fixed lattice constant.

In spite of the fact, that the qualitative feature of the band structure in all the Brillouin zone is very similar for the two compounds, the magnitudes of the two internal gaps for both alloys under the same conditions, as stated in the Tables VI and VII are, as expected, quite different. It is worth saying that these differences could be important in the efficiency of the solar cells built with this material. However they are not far from the optimal values calculated by Luque and Martí.[1] For instance, the magnitudes of the indirect total band gap including the value of the intermediate bandwidth in the cases of SZ-GGA/DZ-GGA ($n=2/6$) have values of $\Delta E_{VC}=1.82/1.79$ eV for Ga_4As_3Ti and $\Delta E_{VC}=2.16/2.12$ eV for Ga_4P_3Ti. In particular these latter values are very close to the gap values corresponding to the maximum of the efficiency curve.

Moreover Cuadra, Martí, and Luque[34] have developed a procedure for the calculation of the efficiency of a solar cell in theoretically ideal conditions. They have applied this method to the data stated in Tables VI and VII of this paper and found efficiencies close to 42% for Ga_4As_3Ti and 46% for Ga_4P_3Ti in a DZ-GGA calculation.[35] These estimations are far from the potential limiting efficiency that a solar cell of 63.2% proposed for the authors could reach but the theoretical enhancement achieved with these specific materials with a metallic intermediate band with these first calculations is significant.

TABLE VII. Energy properties convergence versus basis set size in GGA calculations for $TiGa_4P_3$. Same legend as in Table IV.

n	Basis set(Ti/Ga/P)[a]	ΔE_{VI}	ΔE_I	ΔE_{IC}	ΔE_{VC}	ΔE_{FV}
1	SZ/SZ/SZ[b]	0.72	1.13	0.94	2.79	1.75
2	SZ/SZ/SZ	0.47	0.87	0.82	2.16	1.28
3	SZP/SZ/SZ	0.47	0.87	0.75	2.11	1.29
4	SZP/SZP/SZP	0.59	0.85	0.35	1.79	1.37
5	DZP/SZP/SZP	0.42	0.89	0.45	1.88	1.36
6	DZ/DZ/DZ	0.38	1.06	0.68	2.12	1.37
7	DZP/DZ/DZ	0.39	1.06	0.68	2.13	1.37

[a]SZ: single ζ; DZ: double ζ; SZP: SZ with polarization; DZP: DZ with polarization

[b]Calculation performed with fixed lattice constant.

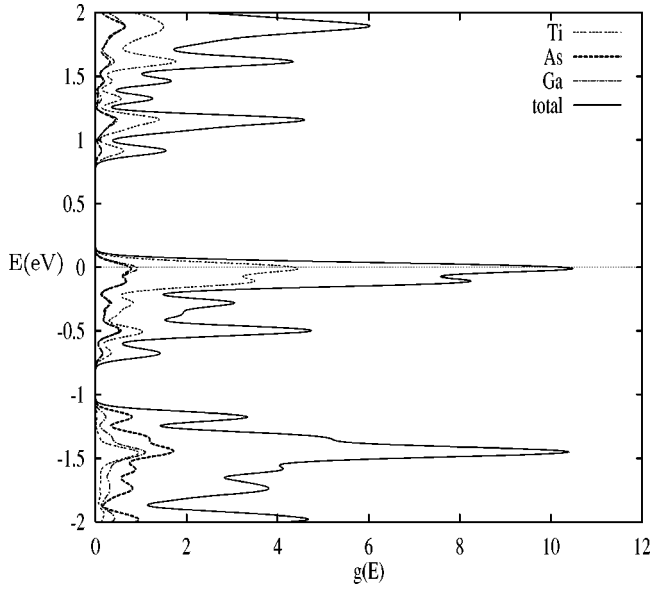

FIG. 7. Total density of states for $TiGa_4As_3$ for the DZP-GGA calculation, is shown for every band. Projected density over each atom is stated as dotted curve for Ti atom, dashed-dotted line for Ga atom, dashed line for As atom and simple line for total density of states.

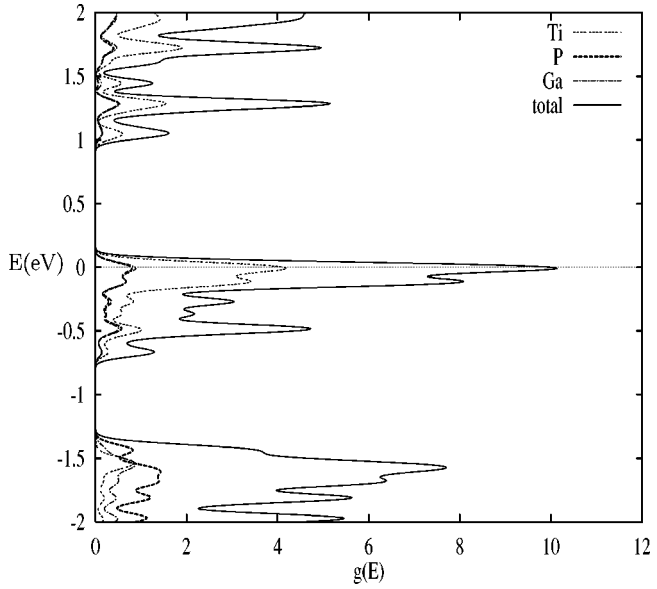

FIG. 8. Total density of states for $TiGa_4P_3$ for the DZP-GGA calculation, is shown curve for every band. Projected density over each atom is stated as dotted curve for Ti atom, dashed-dotted line for Ga atom, dashed line for P atom, and simple line for total density of states.

C. Density Analysis

To explain the formation of the IB, the systems we are interested in could be visualized in our study as a substitution of one impurity atom (Ti) in the zinc-blende crystal structure of the parent semiconductors AsGa or PGa. In the parent semiconductors one Ga atom is surrounded by four As (P) atoms in a tetrahedral disposition and vice versa. In the case of an impurity-isolated defect, a density-functional study[36] shows the situation where one As atom replaces the position of one Ga atom, giving one extra filled orbital in the vicinity of the defect whose state energy appears to be separated in the band gap. However, if one of the As (or P) sites becomes occupied by a Ti atom with four valence electrons, one open-shell orbital localized in its proximity will be produced and the single-particle energies could appear in the semiconductor band gap, separating both occupied and unoccupied orbitals. This situation could be produced with a Ti atom because of the localized character of the *d* electrons. If this substitution appears in the whole crystal, it could give rise to an intermediate band instead of a state. The characteristics of the interactions between the atoms and the overlapping of the orbitals in the suitable directions will define the possibility of the narrow and isolated band formation.

To analyze the composition of the atomic components of the half filled intermediate band formed, we show the density of states for the two alloy-systems, Ga_4As_3Ti and Ga_4P_3Ti in Figs. 7 and 8. The figures summarize the total density of states as calculated with the DZP-GGA correction for each system, and the partial density obtained after projecting the total density on each atom. We represent the energy zone corresponding to the IB and the edges around the gap of the VB and the CB. The two band gaps of the compounds appear well defined in these representations. Results are very similar for the two systems especially near the zero energy where Fermi level is situated. These narrow bands present a metallic character and are made up mainly of orbitals coming from Ti atoms.

A closer inspection of the atomic-orbital composition of the three states responsible for these isolated narrow bands: 14, 15, and 16, near the high symmetry *K* point in the $K \rightarrow \Gamma$ main direction of the Brillouin zone, have been made for the two alloys. We choose this specific point because in the energy diagrams (Figs. 4 and 5), the IB has its largest width. The inspection reveals that for both alloys, only two of the six valence orbitals of Ti, the d_{xz}, and d_{yz}, make significant contribution to the formation of the metallic IB. For the two higher states in the IB near the Fermi level, the 15 and 16 states, the calculations show that the d_{yz} and d_{xz} orbitals of Ti have the most important orbital weight to these states, in a proportion close to 50%. The main overlapping of the *d* orbitals bonding with the corresponding components of the *p* orbitals of Ga and As (or P) atoms are in these directions.

However, state number 14, the deepest in the IB, is formed near the *K* point mainly by the *s* orbital of the Ti (with spherical symmetry) bonding with several components of the *p* orbital of Ga and As (or P) atoms, in both systems. On the other hand, an analysis of the first empty state, number 17, shows that the d_{xy} orbital of Ti, is the main contribution to the formation of this state, with a weight close to 73% in this symmetry point. This means that near *K* point the first empty state of each conduction band exhibits a strong Ti $3d$ character.

Quantitatively, this situation is slightly different if we analyze the atomic-orbital components of these states in the average of all directions in the Brillouin zone for the IB, al-

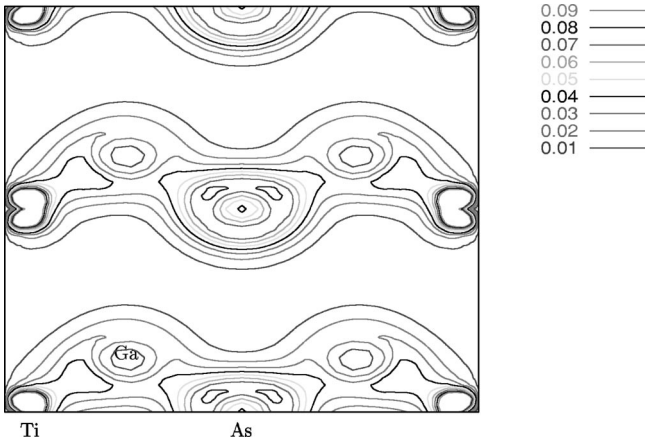

FIG. 9. Total density distribution of electronic charge for $TiGa_4As_3$ (electrons/Å^3) for the case of DZ-GGA used, displayed for (110) lattice plane.

though qualitatively it is quite similar. We note that for the two higher partially occupied 15 and 16 states, the three components of the d orbitals d_{xy}, d_{xz}, and d_{yz}, are involved, in with a total weight of Ti atom which is slightly less, especially in the case of Ga_4As_3Ti. However the first empty state in each conduction band has an orbital weight of Ti close to 40%, much smaller than in the previous specific point in the Brillouin zone close to the K main point. This feature gives therefore, a hybrid $3d$-$4p$ state made up of Ti as well as Ga and As (or P) for this first empty state.

The total density distribution of the electronic charge in the calculated DZ-GGA corrections, for the two systems Ga_4As_3Ti and Ga_4P_3Ti, are shown in Figs. 9 and 10, respectively, for the (110) lattice plane. Contour lines of the total density show the polarization of the electronic charge in the bonding between Ti and Ga and Ti and As (or P). In this plane, the corresponding bond lengths obtained after atomic relaxation, give the values of 2.66 Å for Ti-Ga and 2.56 Å for P-Ga in the case of Ga_4TiP_3, and 2.91 Å for Ti-Ga and 2.85 for As-Ga in the case of Ga_4TiAs_3. These values show that the Ti atom, does not cause much distortion in the crystal structure in particular when Ti substitutes the P atom. Mulliken population analysis shows that the charge transferred from the Ti atom to the other atoms is about 1.06 e in both compounds. However, there is a substantial redistribution of this charge among the other seven atoms surrounding the Ti, with a final charge of 0.17 for Ga/0.125 for As and 0.11 for Ga/0.20 for P, respectively, suggesting the formation of the covalent bonding. Figures 9 and 10 show also the formation of a directional covalent bonding between the atoms in this plane for both compounds. There is a fairly strong p-d interaction between the Ti and the Ga and As (or P) layer in the (110) lattice plane confirming what we previously inferred from the quantitative study of the density of states (DOS) in the average Brillouin zone.

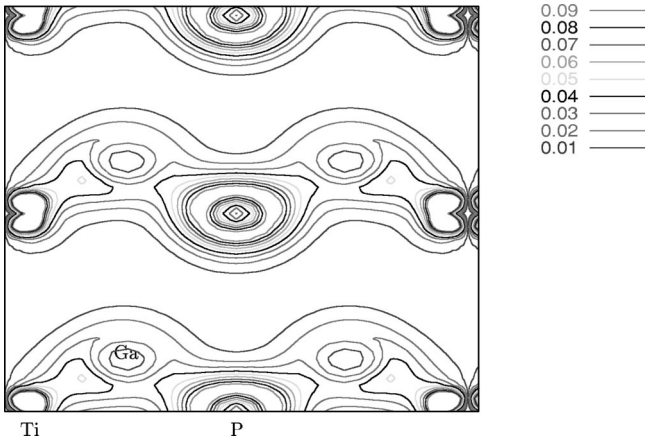

FIG. 10. Total density distribution of electronic charge for $TiGa_4P_3$ (electrons/Å^3) for the case of DZ-GGA used, displayed for (110) lattice plane.

IV. CONCLUSION

The dynamically atomic relaxed alloy semiconductor compounds Ga_4As_3M and Ga_4P_3M with M = Sc, Ti, V, and Cr, have been investigated using the first-principles total-energy calculation and a periodic eight-atom cubic cell. In particular, more detailed studies using the LDA-DFT and the GGA-DFT correction methods and basis set convergence, have been carried out for Ga_4As_3Ti and Ga_4P_3Ti systems. We have found an intermediate narrow band, stable and with metallic character, formed between the valence band and the conduction band in all cases studied for both compounds. These intermediate metallic bands are well localized in the two compounds and characterized in the whole Brillouin zone by the determination of the structural and energy parameters. We found that the IB is related to the valence band by a direct transition band gap and with the conduction band by an indirect transition band gap in both systems.

To investigate the atomic composition of the states related to the formation of the IB, an analysis of the total and partial density of states and atomic-orbitals composition of each state have been carried out. We point out that close to half of the atomic population of the intermediate band higher states are Ti in both compounds. Moreover, the total density distribution displayed for the (110) lattice plane shows an important interaction between the Ti and Ga and As (or P).

On the other hand, it is well known that the band gap obtained by the Kohn-Sham eigenvalues in the local-density approximation and in the generalized gradient correction are not given accurately, because they do not represent the excitation energies well. We believe that our results for the band-gap energies summarized in Tables IV to VII are slightly underestimated. A comparison of the corresponding experimental energy band gaps of the parent semiconductors AsGa/PGa[37] with those calculated for the same systems gives always lower values for calculations in all cases. For instance, calculations made for AsGa/PGa with DZP-GGA(LDA) corrections give band-gap energies of 0.45/1.46 (0.99/1.56) eV compared to 1.52/2.35 eV for experimental band-gap energies and 1.17/2.44 eV for calculations made with an GW method.[37] Because of the limitations of DF theory, further extension of the calculations beyond LDA and GGA such as the exact exchange and the quasiparticle method is needed to estimate band-gap corrections and de-

termine real excitation spectra. From our studies we can predict that the solar efficiency of conventional Si solar cells could be increased significantly with this type of material.

ACKNOWLEDGMENTS

We wish to thank Professor A. Luque for his enthusiastic discussions and for a critical reading of the manuscript and Professor J. C. Conesa for his support and active discussion during this work. The authors would also like to thank Professor A. Martí, Professor F. Flores, and Professor J. Ortega, for fruitful discussions. We are indebted to E. Artacho, P. Ordejon, D. Sanchez-Portal, J. M. Soler, and A. Garcia for providing us the SIESTA computational code. This work was partially supported by Spain's Plan Nacional de I+D and FEDER programs under references TIC2000-1339-C02-02 and 2FD97-0332-C03-01, the European Commission Contract No. ENK6 CT200 00310, and by Universidad Politécnica de Madrid under Grant No. 011188.

[1] A. Luque and A. Martí, Phys. Rev. Lett. **78**, 5014 (1997).
[2] W. Shockley and H. Queisser, J. Appl. Phys. **32**, 510 (1961).
[3] A. Luque and A. Martí, Prog. Photovoltaics **9**, 73 (2001).
[4] A. Luque, F. Flores, A. Martí, J. C. Conesa, P. Wahnón, J. Ortega, C. Tablero, R. Pérez, and L. Cuadra, ''Intermediate Band Semiconductor Photovoltaic Solar Cell,'' U.S. Patent No. WO 00/77829 published by International Bureau of WIPO on 21.12.2000.
[5] P. Wahnón, J. Fernández, and C. Tablero, in Proceedings of Psi-K 2000 Conference: ''*Ab initio (from electronic structure) calculation of complex processes in Materials*'' (Schwäbisch Gmünd, 2000), p. 96.
[6] R. G. Parr and W. Yang, *Density Functional Theory of Atoms and Molecules* (Oxford, New York, 1989).
[7] J. F. Dobson, G. Vignale, and M. P. Das, *Electron Density-Functional Theory. Recent Progress and New Directions* (Plenum, New York, 1998).
[8] SIESTA is a very efficient LCAO code program, specially designed to perform standard DFT calculations by direct diagonalization, or using order-N algorithms suitable for very large systems. P. Ordejón *et al.*, Phys. Rev. B **53**, R10441 (1996); D. Sanchez-Portal *et al.*, Int. J. Quantum Chem. **65**, 453 (1997); E. Artacho *et al.*, Phys. Status Solidi B **215**, 809 (1999) and references therein.
[9] To our knowledge, the only investigations carried out related to these systems have been geared to the study of phase equilibria at high temperatures for diffusions and reactions at interfaces in Ti-AsGa and Pt,Ti-AsGa ohmic contacts. Unfortunately, no Ti-Ga-As ternary alloy was identified in these studies. R. Schmid-Fetzer, J. Electron. Mater. **17**, 193 (1988); Q. Han and R. Schmid-Fetzer, METALL **46**, 45 (1992); K. A. Whitmire *et al.*, J. Mater. Sci.: Mater. Electron. **9**, 357 (1998) and references therein.
[10] P. Hohenberg and W. Kohn, Phys. Rev. B **136**, 864 (1964).
[11] W. Kohn and L.J. Sham, Phys. Rev. **140**, 1133 (1965).
[12] D.M. Ceperley and B.J. Alder, Phys. Rev. Lett. **45**, 566 (1980).
[13] J.P. Perdew and A. Zunger, Phys. Rev. B **23**, 5048 (1981).
[14] A.D. Becke, J. Chem. Phys. **85**, 7184 (1986); Phys. Rev. A **38**, 3098 (1988).
[15] D.C. Langreth and J.P. Perdew, Phys. Rev. B **21**, 5469 (1980).
[16] J.P. Perdew, Phys. Rev. B **33**, 8822 (1986).
[17] M. Levy and J.P. Perdew, Phys. Rev. B **48**, 11 638 (1993).
[18] J.P. Perdew, K. Burke, and M. Ernzerhof, Phys. Rev. Lett. **77**, 3865 (1996); **78**, 1396 (1997).
[19] K. Burke, J. P. Perdew, and Y. Wang, in *Electron Density Functional Theory. Recent Progress and New Directions*, edited by J. F. Dobson, G. Vignale, and M. P. Das (Plenum, New York, 1998), p. 81.
[20] N. Trouiller and J.L. Martins, Phys. Rev. B **43**, 1993 (1991).
[21] L. Kleinman and D.M. Bylander, Phys. Rev. Lett. **48**, 1425 (1982).
[22] D.M. Bylander and L. Kleinman, Phys. Rev. B **41**, 907 (1990)
[23] O.F. Sankey and D.J. Niklewski, Phys. Rev. B **40**, 3979 (1989).
[24] D. Sanchez-Portal, E. Artacho, and J.M. Soler, Solid State Commun. **95**, 685 (1995).
[25] A.A. Demkov, J. Ortega, O.F. Sankey, and M.P. Grumbach, Phys. Rev. B **52**, 1618 (1995).
[26] S. Huzinaga, *Gaussian Basis Set for Molecules Calculations* (Elsevier, Amsterdam, 1984).
[27] W.J. Hehre, R. Ditchfield, and J.A. Pople, J. Chem. Phys. **56**, 2257 (1972).
[28] W. A. Harrison, *Electronic Structure and the Properties of Solids*, (Dover, New York, 1989).
[29] A. Garcia, C. Elsässer, J. Zhu, S.G. Louie, and M.L. Cohen, Phys. Rev. B **46**, 9829 (1992).
[30] M. Springborg, in *Density Functional Theory*, edited by P. Geerlings, F. de Proft, and W. Langenaeker (VUB University Press, Brussels, 1999), p. 39.
[31] M. Fuchs, M. Bockstedte, E. Pehlke, and M. Scheffler, Phys. Rev. B **57**, 2134 (1998) and references therein.
[32] S. M. Sze, *Physics of Semiconductors Devices*, 2nd ed. (Wiley, New York, 1981), p. 848.
[33] W.G. Aulbur, L. Jönsson, and J.W. Wilkins, Solid State Phys. **54**, 1 (1999).
[34] L. Cuadra, A. Marti, and A. Luque, in 16*th* European Photovoltaic Solar Cell Energy Conference (Glasgow, UK, 2000).
[35] A. Marti, L. Cuadra, and A. Luque (private communication).
[36] D.J. Chadi and K.J. Chang, Phys. Rev. Lett. **60**, 2187 (1988).
[37] K.A. Johnson and N.W. Ashcroft, Phys. Rev. B **58**, 15 548 (1998).